Cometary Spectroscopy

Nicolas Biver

LESIA, UMR8109 du CNRS, *Observatoire de Paris-Meudon*, 5 Place Jules Janssen, 92195 Meudon Cedex, France
Email: nicolas.biver@obspm.fr

Abstract. Cometary spectroscopy from the ultraviolet to the radio wavelength domain provides us with insights on the composition of the gases that are released by the cometary nuclei. While infrared to millimeter spectroscopy give access to the parent molecules that are released directly from the nucleus, visible spectroscopy enables observation of daughter species. Those "radicals" observable in the visible domain have more complex spectroscopic band-like structures and are mainly CN, C_2, C_3, NH_2. Their spectroscopic signatures are easily accessible to amateur astronomers class equipment. Provided that carefully calibrated data are acquired, some simple calculation can readily be done to convert the line intensities into comet molecular outgassing rates and thus provide interesting physical data on comets. In addition to broadband dust measurements, the interested amateur can produce valuable scientific data on comets that will always be welcome from the professional community and certainly useful as the monitoring of comets activity is always essential.

1 Introduction

Spectroscopic study of comets provides information on the physical and chemical characteristics of the coma surrounding their nucleus. Molecules sublimating from the nucleus ("parent molecules") and their photo-dissociation products have narrow spectral signatures in the ultraviolet to visible, infrared and radio wavelengths domains, depending on the emission mechanism. Very high spectral resolution ($\lambda/\Delta\lambda \geq 10^6$) is necessary to get information on the gas expansion velocity. Only radio techniques can provide it (Figs. 6–8). On the other hand, wide band spectroscopy can show the emission spectrum of dust in the mid- to far- infrared (5-100μm) domain (Figs. 1, 3) and the scattered sun light in the visible range (Figs. 1, 2).

In the ultraviolet-visible domain, cometary spectra are dominated by spectral lines of radicals, unstable molecules which come from parent molecules which have been stripped of one or a few atoms by the solar radiation. The main radicals are C_2, responsible for the famous cometary "Swan bands" and the green tint of cometary comae, CN (violet), C_3, NH, NH_2 and OH (Fig. 2). Line intensities are used to determine the amount of molecules in the coma. On the other hand, the integrated intensity of the continuum can be used to estimate the quantity of dust in the coma but strongly depends on its physical characteristics: size distribution of grains, scattering properties,...

We will start with an inventory of comet molecules and investigation techniques before focusing on the analysis of visible comet spectra which is a discipline accessible to amateur astronomers.

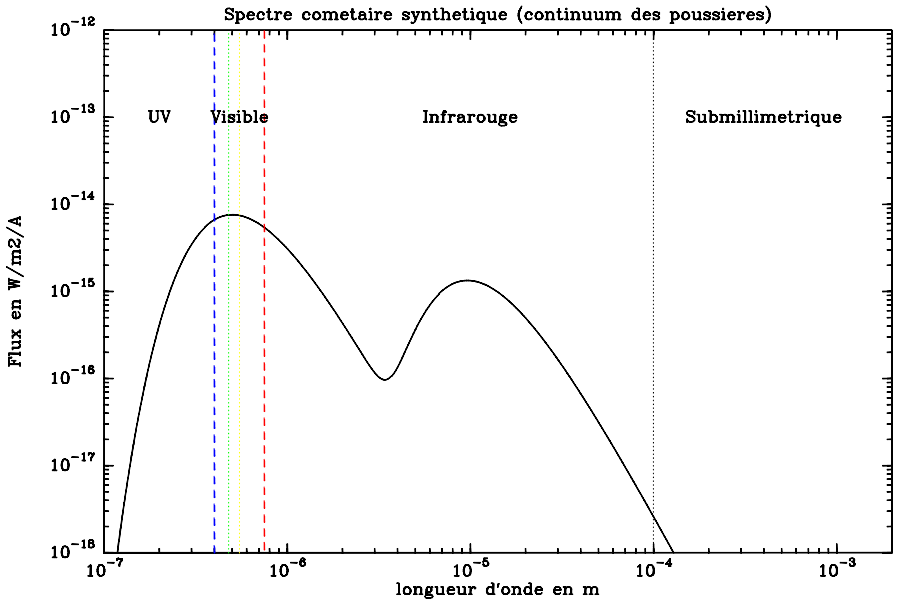

Fig. 1. Very wide band (UV to radio) synthetic spectrum of a bright comet. Please provide figure in English.

2 The observation of cometary molecules

The main specificity of cometary nuclei is to be composed of a large fraction of ices of volatiles such as water but also CO and CO_2, for the main components. As the comet nucleus gets close to the sun its ices sublimate to create the cometary atmosphere (coma) and tails of ionized gas and dust. Dust comes out from the nucleus leveled off by the gas.

Although water has been suspected as the major component of cometary ices for over a century, it was only directly observed for the first time in 1986. However, the visible signatures (Fig. 2), C_2 green SWAN bands, CN cyanogen line (The presence of cyanogen in comets was responsible for the 1910 panic at the time the earth crossed Halley's comet tail) and atomic lines seen in sun-grazing comets have been identified for over a century. But these only trace decomposition products of the main "parent" molecules coming directly from the nuclear ices sublimation. Radio and infrared techniques are the ones responsible for the identification of over 22 parent cometary molecules between 1985 and 1997 (Table 1).

Fig. 2 and 3 give an overview of typical comet spectra with both continuum and spectral lines. After the inventory of cometary lines, we will look at the different techniques and frequency ranges to observe these cometary molecules.

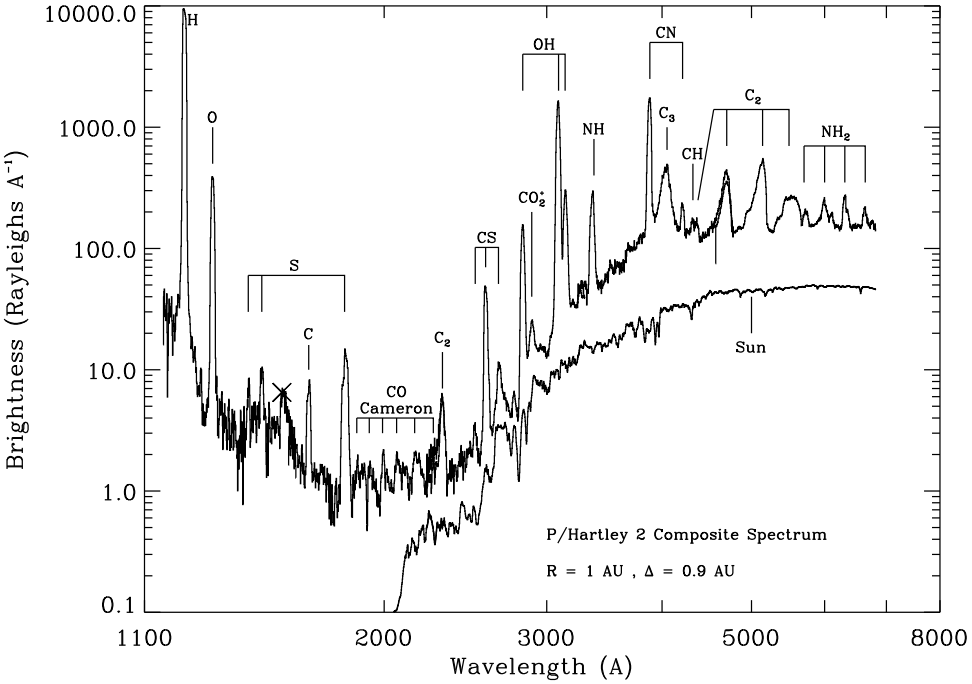

Fig. 2. Ultraviolet to visible spectrum of comet 103P/Hartley-2 observed with the Hubble Space Telescope [26],[13]. In addition to the classical visible radical and ion bands on the right, in the UV one can notice atomic lines and the strong H Lyman-α line at 1216 Å. Atomic hydrogen, mostly coming from the photo-dissociation of water, is the most abundant species in cometary comae.

2.1 The observed cometary molecules

Table 1 hereafter provides the list of the majority of molecules and radicals observed in comets, their mean relative abundance to water, and parent scale-length (L_p) for a photo-dissociation product and dissociation scale-length (L_d) that will be useful to evaluate their production rate and abundance (Section 4). Scale-lengths are given at an heliocentric distance r_h of 1 AU, and often scale as r_h^2. Several radicals are photo-dissociation products of well known parent molecules, such as:

- $H_2O \rightarrow$ OH, H;
- HCN $\rightarrow$ CN;
- C_2H_2, $C_2H_6 \rightarrow C_2$;
- $NH_3 \rightarrow NH_2$, NH

Table 1. Observed cometary molecules

Molecule	Main lines			Abundance	Scale-lengths at 1 AU	
	Radio	Infrared	Visible - UV	[% water]	L_p [km][d]	L_d [km][d]
H_2O	0.54-0.17mm[1]	2.7, 6.3μm[a], 1.94, 2.95μm 4.65μm	–	100	0	70000
OH	18 cm	2.87μm[a] 3.04,3.28μm	0.30μm	90	25000	160000
H	–	–	121.6nm[a]	200	$\approx 10^5$	$3\ 10^7$
CO_2	–	4.25μm[a]	(from CO[b]:) (185-230m[a])	5–10	0	430000
CO	2.6-0.65mm	4.67μm	142-160nm[a]	1–25	0+	$1.3\ 10^6$
CH_4	–	3.31μm	–	0.2–0.8	0	105000
C_2H_2	–	3.03μm	–	0.3	0	60000
C_2H_6	–	3.35μm	–	0.1–0.7	0	75000
C_2	–	–	0.45-0.56μm	0.01–0.70	20000	70000
C_3	–	–	0.405μm	0.003–0.07	2500	20000
CH	–	3.35μm	0.431μm	0.05–0.5	80000	5000
CH_3OH	3–0.6mm	3.52μm	–	0.5–6	0	60000
H_2CO	2.1–0.8mm	3.59μm	–	0.1–1.2	7500	5000
HCOOH	1.3mm	–	–	0.09	0	27000
CH_3CHO	2–1mm	–	–	0.02	0	12000
$HCOOCH_3$	1.3mm	–	–	0.08	0	18000
$(CH_2OH)_2$	3–1mm	–	–	0.25	0	10^5?
NH_3	1.3cm	3.00μm	–	0.7	0	5500
NH_2	–	3.23μm	0.52-0.74μm	0.2	5000	10000
NH	–	–	0.336μm	0.3	50000	150000
HCN	3.4–0.4mm	3.0μm	–	0.08–0.25	0	57000
CN	1.3mm	4.90μm	0.388μm	0.1–0.6	20000	200000
HNC	3.3–0.8mm	–	–	0.005-0.02	0 ?	57000
HNCO	1.4–0.9mm	–	–	0.1	0	29000
CH_3CN	3.3–1.3mm	–	–	0.01	0	110000
HC_3N	3.3–1.1mm	–	–	0.01	0	13000
NH_2CHO	1.3mm	–	–	0.01	0	10^4?
H_2S	1.8, 1.4mm	–	–	0.4-1.5	0	4000
OCS	2.0–1.0mm	4.86μm	–	0.4	0+	9000
CS (CS_2)	3.1–0.9mm	–	260nm	0.1	300	40000 ?
SO_2	1.5–1.3mm	–	–	0.2	0	4000
SO	1.4–1.0mm	–	–	0.3	4000?	6000
H_2CS	1.3mm	–	–	0.02	0	?000
NS	0.9mm	–	–	0.02	?	?
S_2	–	–	290nm	0.005	0 ?	200
H_2O+		3.1μm	550-747nm	0.2%($r_n = 10^5$)–2%($r_n = 10^6$km)		
H_3O+	1.0mm	2.8μm	–	0.01% maxi at $r_n = 10^4$km[c]		
CO+	1.3mm	-	340-630nm	0.1%($r_n = 10^5$)–30%($r_n = 10^6$km)		

[a] *non observable from the ground;*
[b] *photo-dissociation product of CO_2 in an excited state;*
[c] *r_n = distance from comet nucleus in km;*
[d] *using $v \approx 0.8$ km/s for life-time to scale-length conversion when possible.*

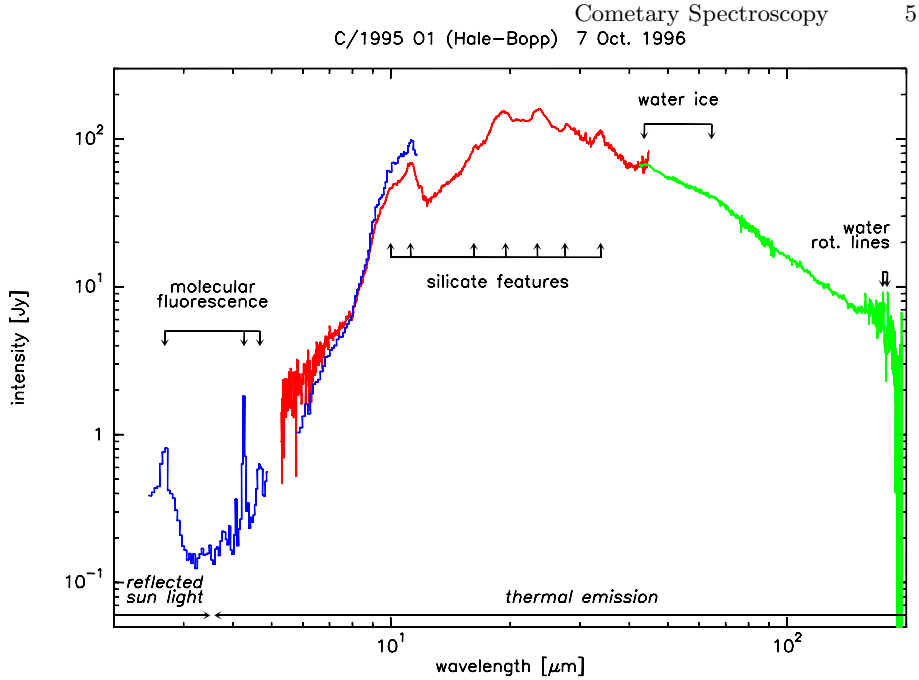

Fig. 3. Near to far infrared spectrum of comet C/1995 O1 (Hale-Bopp) observed with the Infrared Space Observatory [11]. In addition to the blackbody spectrum of the dust, several silicate emission bands appear in the middle of the spectrum. On the other hand a few molecular lines are seen on each side (left: vibrational bands, right: rotational lines) of the spectrum.

3 Comets molecular spectroscopy

3.1 Short introduction to molecular spectroscopy

The purpose of this section is not to make a detail presentation of the principles of molecular spectroscopy, but just give some simple basics and examples to understand the difference between different wavelength spectra. Generally the wave function describing a molecule state is made of 3 main components: electronic function, vibrational function and rotational function. The last two functions are not relevant to isolated atoms. In most cases (because of high energy differences) those 3 functions can be decoupled, and the total molecular energy will be the sum of electronic plus vibrational plus rotational energies (from the highest to lowest), which are all quantified and can be estimated from a number of quantum numbers.

To the first approximation each energy mode can be studied independently and the coupling between modes will not change significantly the energy levels. We will look at the case of the CO molecule, abundant in comets and one of the

simplest example. Generally the complexity and lack of symmetry of a molecule will make the spectra more complex and require a larger number of quantum numbers to describe the energy states. They can be even further more split into energy sub-levels (especially for radicals) and lead to more complex hyperfine spectral structures.

- Rotational states can be described by 1 to 3 (general case) quantum numbers (e.g. J, Ka, Kb): linear molecules will need one quantum number J, symmetric ones 2, and others 3. In the case of linear molecules, the rotational energy is to first order proportional to $J(J+1)$ (Fig. 4) and thus the frequency of the $J \rightarrow J-1$ rotational state transition is proportional to $2 \times J$. Only the $\Delta J = 0, \pm 1$ transitions are allowed.

- Vibrational states: the more atoms the molecule has, the larger the number of vibrational mode it will have: e.g. only one for CO (C–O binding elongation), 3 for CO_2 or H_2O, 12 for CH_3OH... They are generally called ν_1, ν_2,... and to first approximation the energy level in each vibration mode is proportional to the v quantum number $+1/2$, thus $v = 2 \rightarrow 1$ and $v = 1 \rightarrow 0$ transition will correspond to very similar energy changes and result in spectroscopic lines at close frequencies. But all these vibrational levels have a rotational fine structure and we generally talk about "vibrational bands" since within a given $\Delta\nu$ transition (all allowed) there are many rotational transitions possible. For linear molecules, the $\Delta J = 0, \pm 1$ selection rule results in three different series of lines "P ($\Delta J = +1$), Q($\Delta J = 0$), R ($\Delta J = -1$) branches" – for CO the Q branch is forbidden.

- Electronic states: labeling of the molecular electronic states is done in a similar way to atomic electronic states: they mostly concern energy levels of the outer electron(s). Energies are again much higher than for rotational and vibrational states, but there are often only a few electronic states of interest since other are generally dissociative for the molecule (energy higher than dissociation energy of the molecule). Fig. 5 shows an example of the main two series of electronic levels for CO (with transitions), with their rotational and vibrational fine structure. Vibrational structure has been enlarged for clarity, with respect to the vertical energy scale. This can result in a dense forest of line at high spectral resolution, like in the case of C_2 (Fig. 10) where they are grouped by $\Delta v = 1, 0, -1, -2$ for the vibrational structure transition within the electronic transition – see section 3.4 too.

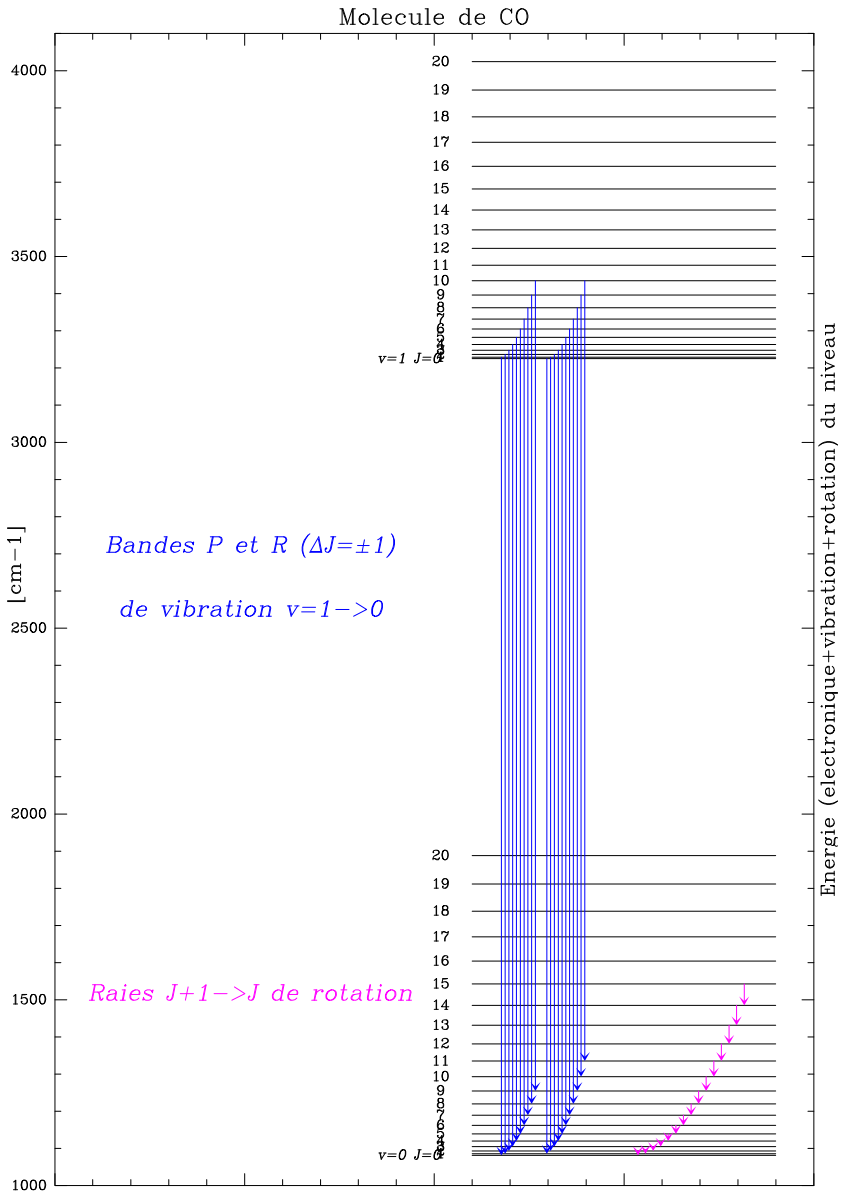

Fig. 4. Rotation states and rotational transition (at right) and first vibration band of CO with its rotational structure an corresponding transitions. Vertical scale: energy level in cm−1. Please provide Figure in English

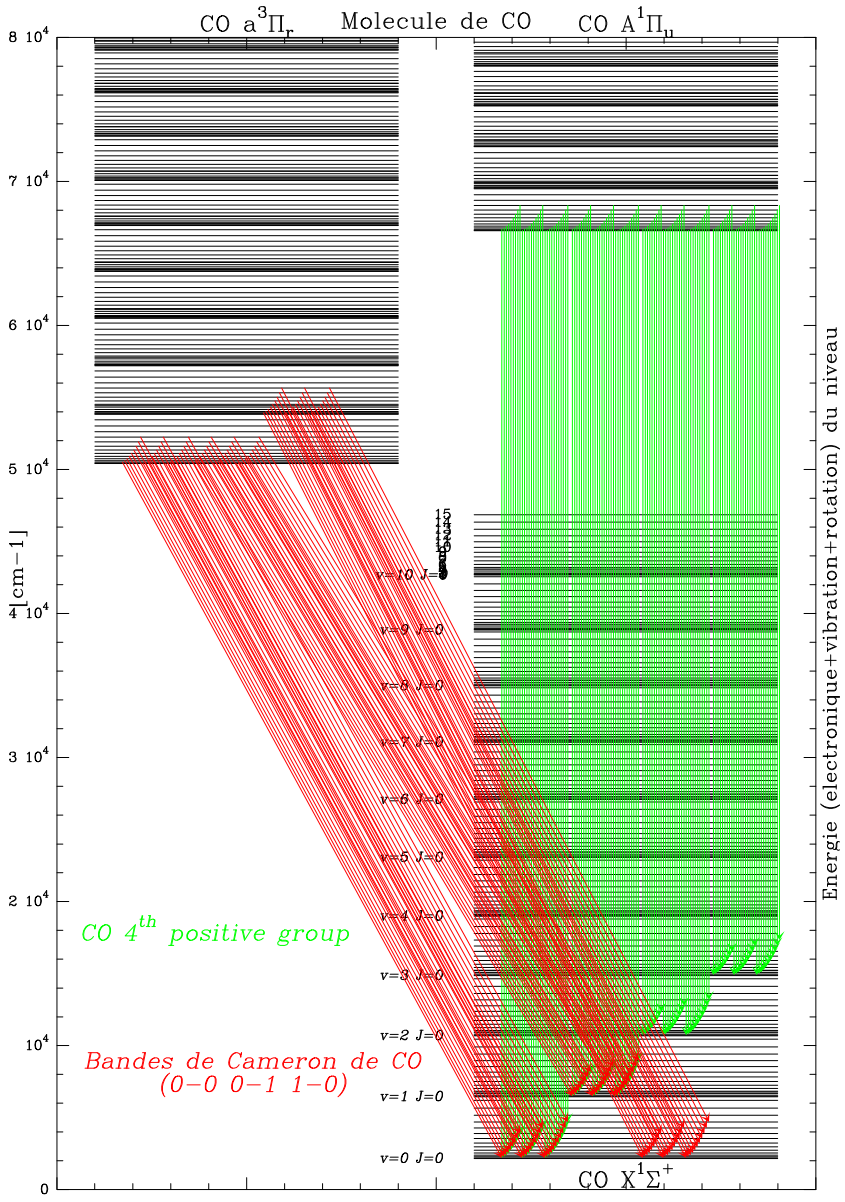

Fig. 5. UV electronic bands of CO. Please provide Figure in English.

3.2 Rotational spectra of molecules

- Spectral domain: radio sub-millimetric to centimetric ($\lambda \approx 0.1$–10mm)
- Observable molecules: all that have a permanent dipole momentum because of their asymmetry (e.g. HCN but not CO_2, nor CH_4)

The interest of this wavelength range is to relatively easily detect parent molecules: the cometary atmosphere is very cold (gas temperatures are in the 10–150 K range) and such lines correspond to transitions between low energy molecular levels. The observation of groups of lines such as those from methanol can probe the gas temperature.

The (radio) heterodyne technique offers access to ultra high spectral resolution (up to 10^8 currently at the Institut de Radioastronomie Millimetrique 30m facility). It can be used to resolve the lines in Doppler velocity. Cometary lines are very narrow ($\Delta\lambda/\lambda \approx 10^{-5}$), since only broadened by the velocity dispersion due to the outgassing geometry. The gas is cold and of very low density and has a mean radial expansion velocity of 0.5 to 1.5 km/s. See example of Doppler-velocity resolved lines in Figs. 6–8 and interpretation.

Lines are usually simple and well separated from each other and no confusion is possible. Over 200 lines have been identified in comets and none is still waiting for identification. There may be a few exceptions but these are marginal features: very weak lines necessitating hours of integration on bright comets with large telescopes (10-30m diameter) at high altitude sites – well beyond amateur capacities.

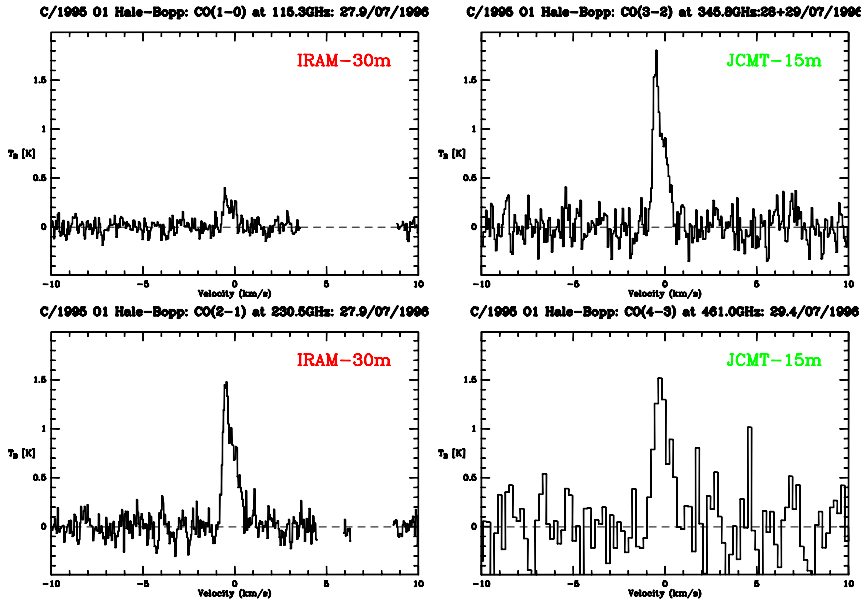

Fig. 6. Radio spectra of the 4 first transitions of CO observed in comet C/1995 O1 (Hale-Bopp) in 1996. The temperature inferred from the relative intensities of the lines was 30K [5]. Transitions are shown in Fig 4.

Usually radio intensity (I) units are converted into temperatures from: $T = \lambda^2/(2k)I$ [Kelvin]. T is the equivalent brightness temperature of the black body that would radiate I (in the Rayleigh-Jeans approximation $\lambda T >> 3000\mathrm{K}\mu\mathrm{m}$).

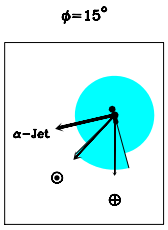

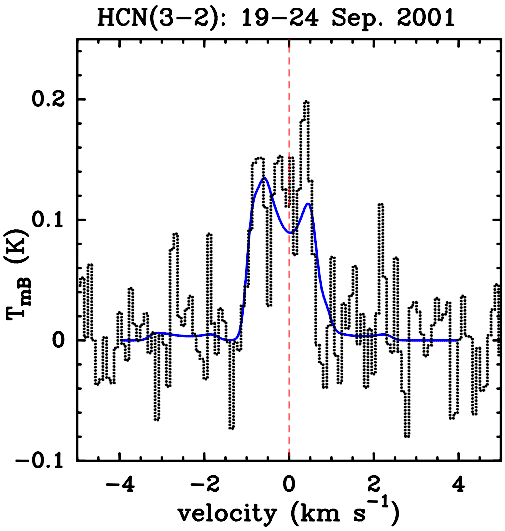

Fig. 7. Radio spectrum of the HCN(3-2) line at 1.1mm in comet 19P/Borrelly in September 2001 observed with the IRAM 30m radio-telescope (doted line). On the left: modeling of outgassing pattern yielding a line profile compatible with observations [6].

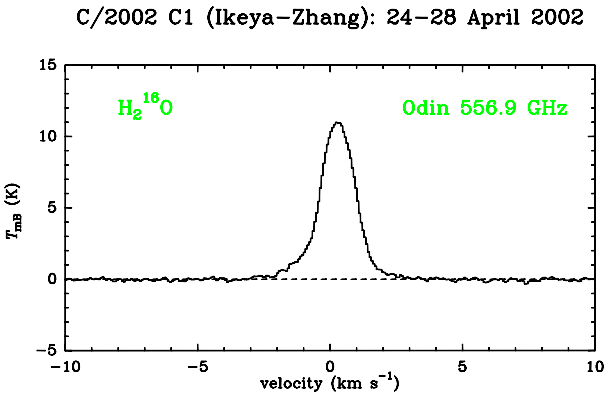

Fig. 8. Spectrum of water at 0.5mm in comet 153P/Ikeya-Zhang from space with the ODIN satellite (1.1m sub-millimeter radio-telescope) [16]. Here, asymmetry is due to self-absorption in an optically thick line.

3.3 Vibrational spectra of molecules

- Spectral domain: infrared ($\lambda \approx 2$–10μm), requiring dry high altitude site;
- Observable molecules: all excepted homo-nuclear molecules such as O_2, N_2 or S_2.

Most molecules are observable in the infrared and a large number can be observed from the ground through atmospheric windows, which namely exclude CO_2 and most of H_2O lines because of telluric absorption. This technique brings the possibility of detecting symmetrical molecules (such as hydrocarbons like CH_4, C_2H_2,...) that have no radio signatures.

The ro-vibrational lines (for a given vibrational transition there is a large number of close transition corresponding to different rotational quantum numbers) are separated at high resolution but can be numerous. In certain wavelength domains, e.g. around 3.4μm, corresponding to the C–H stretching mode of vibration, there can be confusion between several molecules having very close transitions (see Fig 9.). Thus some more complex molecules are more easily identified in the radio. The continuum of the dust (Figs. 1, 3) is also important in this wavelength domain and can be a problem to get a good signal to noise. For a useful resolution ($\Delta\lambda/\lambda > 10\,000$) large optical (3-10m class) telescopes on high altitude sites is necessary.

3.4 Electronic spectra of molecules

- Spectral domain: visible to ultraviolet ($\lambda \approx 0.1$-1μm);
- Observable molecules: atoms, ions, small (2-3 molecules) radicals.

In this domain we mostly only see "daughter" molecules which are only made up of a small number of atoms. Parent molecules have electronic transitions generally weaker as they are at lower wavelength were the Solar flux is weaker and the fluorescence mechanism leading to the line emissions is less efficient. This also occurs at wavelengths corresponding to photon energies which are close to the ones necessary to break (photo-dissociate) apart the molecules, so that most large cometary molecules do not show emission lines in the visible.

In the near-UV to visible we see radicals (CN, C_2, OH, CS) and ions while at shorter wavelength mainly only atoms (H, O, C, Ar): at these wavelength the energy of the solar photons absorbed before spontaneous emission ("fluorescence") is generally larger than any molecular binding and polynuclear species cannot survive.

Spectroscopic fine structure of the electronic transition lines usually gets very complex (see example of CO in previous section) because of the numerous sublevels due to rotational and vibrational structure. Very high resolution is again necessary to fully see this structure (e.g. Fig. 11). Modeling the relative intensity of the fine structure lines of those electronic bands ([20]) can be very complex, especially when there are forbidden transitions (e.g. C_2 section 3.2 and 3.3) that spreads radicals on a very large number of energy levels. The total line strength of each electronic transition is however a bit easier to model, but continuum emission from dust must be properly subtracted to determine line intensities, especially in the case of aperture photometry measurements.

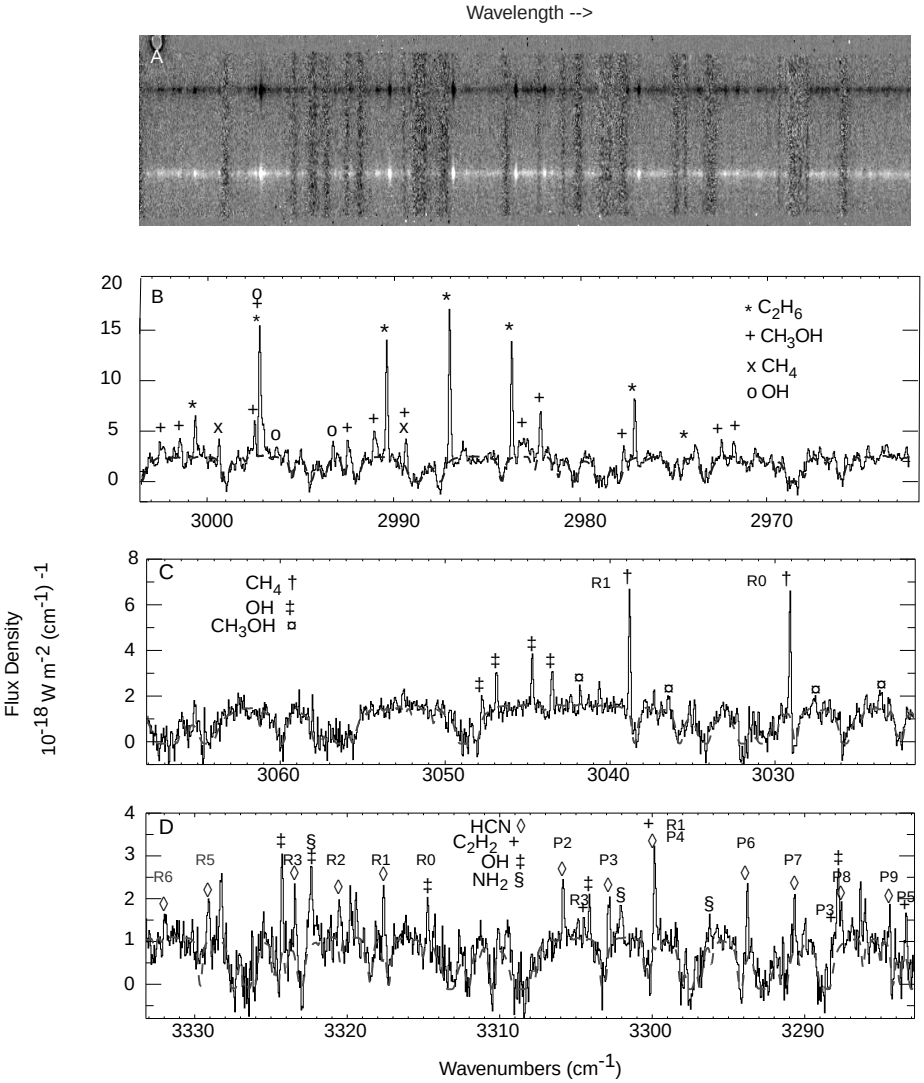

Fig. 9. Infrared spectra of comet C/1999 H1 (Lee) observed with the Keck telescope (and Echelle spectrometer NIRSPEC) [18]. The top plot (A) gives the spectro-image in order 23 with an horizontal cut (B spectrum) below. To cancel atmospheric background, the comet photocenter is moved along the slit from position 1 to 2 (12" above) and the signal subtracted from the previous integration. The full integration results from the "1-2-2+1" series of integration/subtraction to cancel as far as possible atmospheric signal and fluctuations and is repeated as much as necessary to get a good detection. The final result is a positive (white) and negative (black) (A) spectro-image from which spectra are extracted. We can note noisy vertical bands in A corresponding to zero level signal in B, where the atmosphere is opaque and fully absorbs the continuum. An atmospheric transmission profile is overploted in dashed lines on each spectra. C and D correspond to other frequency ranges observed simultaneously in other dispersion orders. The spectral resolution is around 25000.

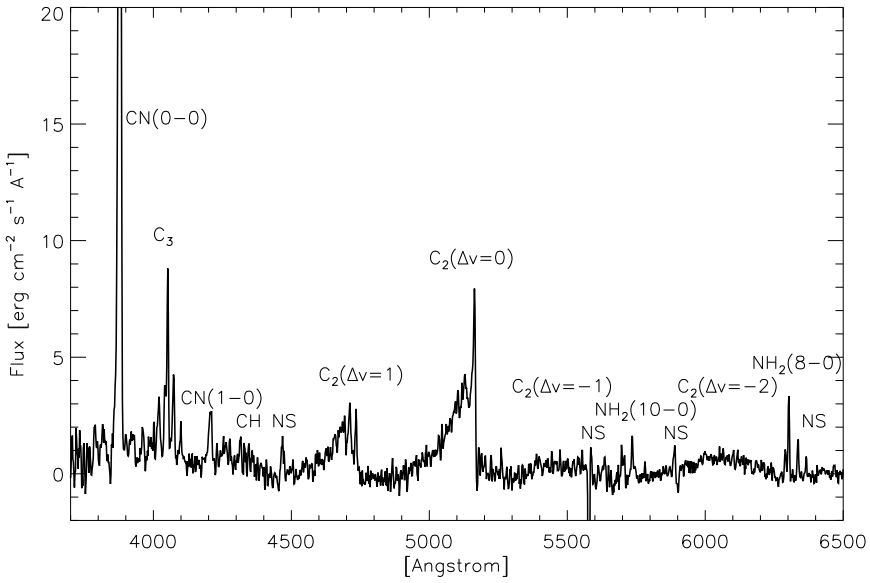

Fig. 10. Visible spectrum of comet C/1995 O1 (Hale-Bopp) obtained with the 1.5m ESO telescope on the 19th of december 1997. Some night sky (NS) lines have only been partially subtracted [19]

Fig. 11. High resolution spectrum ($R \approx 15000$) of the 388nm CN band in comet 1P/Halley in April 1986 [14]. Rotational fine structure becomes clear but even a higher resolution $R = \lambda/\delta\lambda = 70000$ is necessary to isolate each line (This was use to look for ^{13}CN or C^{15}N lines at $R = 83000$ [4]).

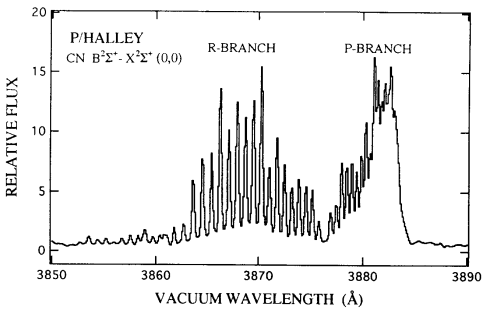

3.5 The main cometary lines in the visible

In contrary to the radio and infrared, this wavelength domain is accessible to many observers, especially amateurs. In addition, there are not that many teams of professional astronomers working on cometary spectroscopy, maybe not much more than 100 around the world.

Table 2. Main visible lines of comets

Molecule	Transition (electronic - vibration band)	wavelength (width)[a]	L/N at 1 AU 10^{-20} W	mean relative intensity
C_2	$d^3\Pi_g - a^3\Pi_u$ Δv=+1	473.7nm(-20nm)	2.40	0.54
C_2	$d^3\Pi_g - a^3\Pi_u$ Δv=0	516.5nm(-30nm)	4.50	1
C_2	$d^3\Pi_g - a^3\Pi_u$ Δv=-1	563.6nm(-30nm)	2.1	0.47
C_2	$d^3\Pi_g - a^3\Pi_u$ Δv=-2	619.1nm(-30nm)	0.7	0.15
C_2	$A^1\Pi_u - X^1\Sigma_g^+$ Δv=+1	1010.0 nm	0.13	0.03
C_2	$A^1\Pi_u - X^1\Sigma_g^+$ Δv=0	1210.0 nm	0.05	0.01
C_3	$A^1\Pi_u - X^1\Sigma_g^+$ $v = 000 - 000$	405.2 nm(35nm)	10.0	0.4
CN	$B^2\Sigma^+ - X^2\Sigma^+$ $v = 1 - 0$	359.0nm (-4nm)		
CN	$B^2\Sigma^+ - X^2\Sigma^+$ $\Delta v = 0$	388.3nm (-4nm)	2.5–4.5[b]	1
CN	$B^2\Sigma^+ - X^2\Sigma^+$ $v = 0 - 1$	421.5nm (-4nm)	≈0.2	0.07
CN	$A^2\Pi_i - X^2\Sigma^+$ $v = 1 - 0$	914.1nm(+15nm)	≈0.7	0.20
CN	$A^2\Pi_i - X^2\Sigma^+$ $v = 0 - 0$	1093.0nm(+15nm)	≈0.9	0.26
CH	$A^2\Delta - X^2\Pi_r$ $v = 0 - 0$	430.5nm (9nm)	0.92	
NH	$A^3\Pi_i - X^3\Sigma^-$ $\Delta v = 0$	336nm (10nm)	0.4–0.9	0.05
OH	$A^2\Sigma^+ - X^2\Pi$ $v = 1 - 0$	282.6nm	0.8–2.7×10^{-3}	0.04
OH	$A^2\Sigma^+ - X^2\Pi$ $v = 0 - 0$	306.4nm (+5nm)	15–83 ×10^{-3}	1
OH	$A^2\Sigma^+ - X^2\Pi$ $v = 1 - 1$	312.2nm (+6nm)	1.2–4.2×10^{-3}	0.07
OH	$A^2\Sigma^+ - X^2\Pi$ $v = 0 - 1$	346.8nm	0.05–0.3×10^{-3}	0.01
NH_2	$A^2A_1 - X^2B_1$ (0,12,0)-(0,0,0)	515 nm	0.551	
NH_2	$A^2A_1 - X^2B_1$ (0,11,0)-(0,0,0)	545 nm	0.279	
NH_2	$A^2A_1 - X^2B_1$ (0,10,0)-(0,0,0)	570 nm	0.299	
NH_2	$A^2A_1 - X^2B_1$ (0, 9,0)-(0,0,0)	600 nm	0.313	
NH_2	$A^2A_1 - X^2B_1$ (0, 8,0)-(0,0,0)	630 nm	0.534	
NH_2	$A^2A_1 - X^2B_1$ (0, 7,0)-(0,0,0)	665 nm	0.175	
NH_2	$A^2A_1 - X^2B_1$ (0, 6,0)-(0,0,0)	695 nm		
NH_2	$A^2A_1 - X^2B_1$ (0, 5,0)-(0,0,0)	735 nm		
Some ion lines, observed far from the nucleus:				
CO+	$A^2\Pi_i - X^2\Sigma^+$ $v = 4 - 0$	379 nm (2nm)		0.8
CO+	$A^2\Pi_i - X^2\Sigma^+$ $v = 3 - 0$	401 nm (2nm)		0.9
CO+	$A^2\Pi_i - X^2\Sigma^+$ $v = 2 - 0$	426 nm (2nm)		1.0
CO+	$A^2\Pi_i - X^2\Sigma^+$ $v = 1 - 0$	455 nm (3nm)		0.7
CO+	$A^2\Pi_i - X^2\Sigma^+$ $v = 2 - 1$	470 nm (3nm)		0.6
CO+	$A^2\Pi_i - X^2\Sigma^+$ $v = 1 - 1$	504 nm (4nm)		0.2
CO+	$A^2\Pi_i - X^2\Sigma^+$ $v = 0 - 1$	549 nm (5nm)		0.5
CO+	$A^2\Pi_i - X^2\Sigma^+$ $v = 0 - 2$	622 nm (6nm)		0.5
H_2O+	$A^2A_1 - X^2B_1$ $v = 0,8,0 - 0,0,0$	616nm		
H_2O+	$A^2A_1 - X^2B_1$ $v = 0,3,0 - 0,0,0$	620nm		
H_2O+	$A^2A_1 - X^2B_1$ $v = 0,2,0 - 0,0,0$	670nm		
OH+	$A^3\Pi_i - X^3\Sigma^-$ $v = 1 - 0$	336nm (-4nm)		
OH+	$A^3\Pi_i - X^3\Sigma^-$ $v = 0 - 0$	362nm (-5nm)		
OH+	$A^3\Pi_i - X^3\Sigma^-$ $v = 0 - 1$	403nm (-4nm)		

[a]: A "-" (resp. "+") sign means that the band extends to shorter (resp. longer) wavelengths from the band head given here;
[b]: $v = 0-0$ alone; multiply by 1.08 to take also into account the $v = 1-1$ band (Others are negligible.) – When L/N varies with heliocentric velocity we give the minimum and maximum values it can reach.

4 Analysis of spectra: computing physical quantities

In this chapter we will not provide the information on how to reduce observational data (cometary spectra) into calibrated scale of intensity units (typically fluxes in [$\mathrm{Wm^{-2}\AA^{-1}}$] or [$\mathrm{Wm^{-2}}$]). It is any observer duty to reduce his data and remove telluric sky lines,... We will describe the basis on how to convert these data into physical quantities characterizing the comet activity, outgassing rate,... as regards to the studied molecules.

4.1 Gas distribution density

This first step is necessary to understand the relationship between the number of molecules observed on the line of sight (Column density N) and the quantity of molecules outgassed by the nucleus every second (Q). To simplify the modeling, we will assume a steady state regime, isotropic coma for the gas and radial expansion at a constant velocity v_{exp}. Variation in those quantities implies additional steps in integration that the interested reader can make.

- Parent molecules are coming directly from the nucleus and destroyed by solar radiation. The photo-dissociation scale-length is Ld ($Ld = v_{exp} \times \tau_d$, τ_d = lifetime, proportional to r_h^2). Then the local density is (Haser model): $n_{\mathrm{molec.}}(r) = \frac{Q_{\mathrm{molec.}}}{4\pi\ r^2\ v_{exp}} exp(-r/Ld)$
- Daughter molecules are not coming from the nucleus but from the destruction of a parent molecule with a scale-length Lp, before being themselves photo-dissociated (scale-length Ld). From this simplistic hypothesis we can define another Haser density profile, using the "Haser equivalent" scale-lengths Lp and Ld): $n_{\mathrm{molec.}}(r) = \frac{Q_{\mathrm{molec.}}}{4\pi\ r^2\ v_{exp}} \frac{Ld}{Lp-Ld}(exp(-\frac{r}{Lp}) - exp(-\frac{r}{Ld}))$

But, e.g., even if HCN → CN by photo-dissociation, Ld(HCN)≠ Lp(CN), because CN is created with an ejection velocity, isotropically when HCN is broken. So the above formula is not using physically representative scale-lengths, but "equivalent scale-lengths" that make the density profile relatively well representative, provided we use the right parameters. A parameter such as Lp(CN) is including several things such as non pure radial trajectory of CN molecules, photo-dissociation of HCN but also possible contribution of other parent molecules (CH_3CN, HNC,...) or other sources. Measuring the Lp and Ld parameters directly from the spectral line intensity spatial profiles in various conditions (heliocentric distance, type of comet,...) is still a useful task.

Data in table 2, with a supposed heliocentric dependence as $1/r_h^2$ are average values given as indicative, and if the observer can re-measure these values to analyze his data, that is better.

The column density will then be (integration on the line of sight at the projected distance ρ from the nucleus):

$$N(\rho) = \frac{2\ Q_{\rm molec.}}{4\pi\ v_{exp}} \frac{1}{\rho} \int_{\rho/Lp}^{\infty} K_0(x)dx$$
$$N(\rho) = \frac{2\ Q_{\rm molec.}}{4\pi\ v_{exp}} \frac{Ld}{Lp-Ld} \frac{1}{\rho} \int_{\rho/Lp}^{\rho/Ld} K_0(x)dx$$

($K_0(x)$: Modified Bessel function, $\int_0^{\infty} K_0(x)dx = \frac{\Pi}{2}$)

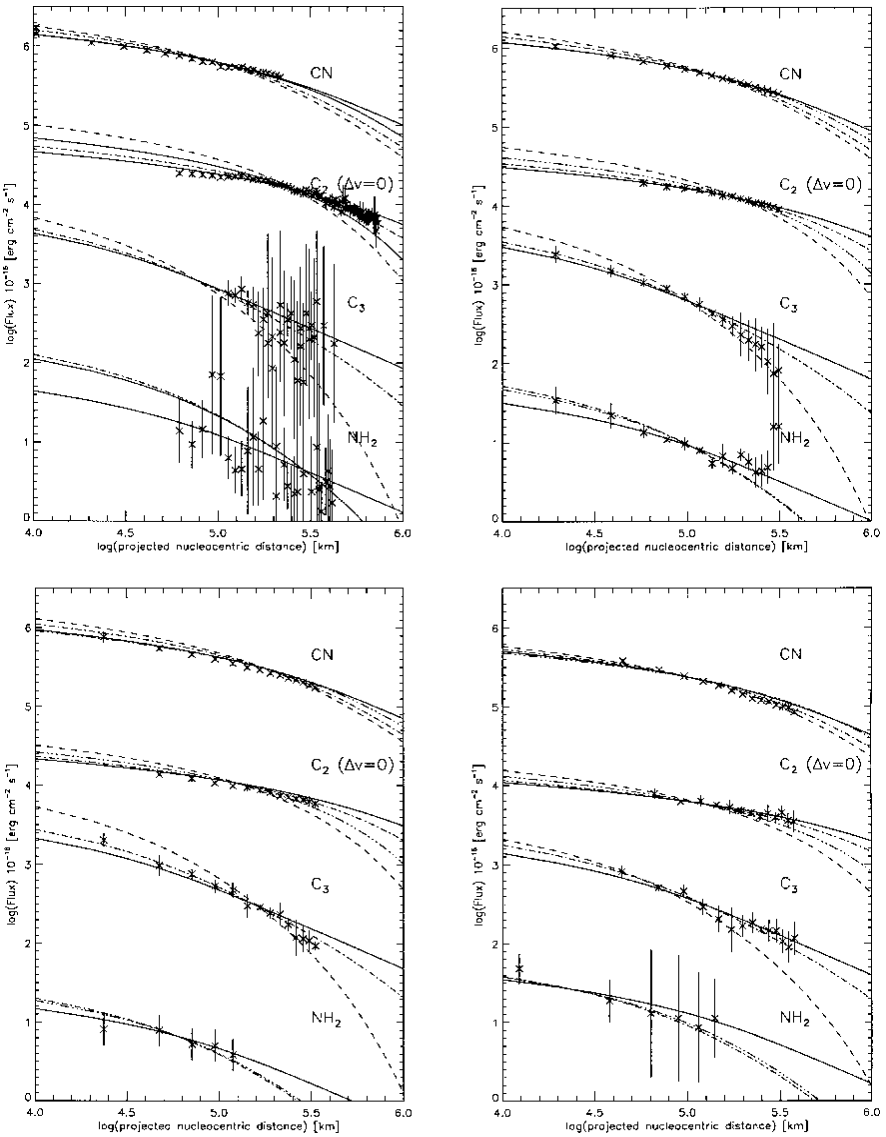

Fig. 12. Radial distribution of lines intensity in the coma of comet C/1995 O1 (Hale-Bopp) for 4 radicals observed (x) in 1997-1998 at ESO. 4 Haser models (lines) have been superimposed (varying Lp, Ld) ([19])

4.2 Molecular "Excitation" (fluorescence process) :

This section will provide information on how to convert a line intensity into a number of molecules. The principle is to know the fraction of molecules that emit photons (of energy $h\nu(\mathrm{j})$) at the $\nu(\mathrm{j})$ considered transition frequency. This involves the Einstein coefficient for spontaneous emission of the transition (A_{ij} [s^{-1}]) and the fraction of molecules in the adequate energy state (i) for this emission to happen.

- For a rotational state/transition: the populating of each rotational state will depend on the distance r to the nucleus, as the collision rate will decrease outwards. This is a complex computation that involves two main different process: collisions and solar radiation pumping.
- For vibrational and electronic transitions (for the global intensity of the bands), the dominating process is called fluorescence: a radiative excitation process in which ground energy state molecule absorbs a photon from the Sun radiation field, followed by a spontaneous emission – following the selection rules than can give a different de-excitation route. Thus, the excitation will not depend on the distance from the nucleus (those processes are much faster than collisions), but the fine rotational structure will, as described above. It will be in many cases an "image" of the ground vibrational/electronic state with its rotational structure that is pumped nearly "as is" to higher vibrational/electronic states, as selection rules mostly only allow slight changes ($\Delta J = \pm 1$) in rotational energy levels through radiative pumping.

One major issue in the UV to visible domain is the complexity of the solar spectrum at these wavelength (many absorption features): the velocity of the comet relative to the Sun ($\dot{r_h}$), due to the Doppler effect, will change the spectrum seen by the comet. The Sun radiation intensity seen by the comet will then depend on its velocity for the narrow window of each molecular lines. Especially for CN, OH and NH ([21],[22],[17]), the pumping rate will strongly depend on the comet velocity (Swings effect).

The variables used to make the conversion between measured flux and column density are:

- F (integrated over the band) is the measured flux [Wm^{-2}];
- $L = 4\pi\Delta^2 F$ total radiated flux in space [Watts = 10^{-7}erg s^{-1}];
- "L/N_{rh}" or $g_r \approx g_0(r_h = 1\mathrm{UA}$ (table 2))$/r_h^2$ is the solar pumping rate of the band (emitted energy in W $\mathrm{molecule}^{-1}$);
- S: cometary atmosphere cross section over which the flux is measured [m^2];
- $\Omega = S/\Delta^2$ corresponding solid angle [steradian];
- N: Molecule column density [molecules m^{-2}];
- r_h and Δ are respectively the heliocentric and geocentric distance of the comet (converted into m).

$$N = \frac{L}{S\ L/N_{rh}} = \frac{4\pi\Delta^2\ F\ r_h^2}{S\ g_0} = \frac{4\pi\ F\ r_h^2}{\Omega\ g_0}$$

4.3 Example

Observation of CN in comet Hale-Bopp on the 19th of December 1997 with the ESO 1.52m telescope: Fig. 10 and 4.3 ([19]):

- Geometry of the observation: r_h = 3.78 AU, Δ =3.63 AU, $\dot{r_h}$= +18.7 km/s
- Other data: v_{gaz} ≈0.65 km/s, Lp ≈300000 km (at 3.8 UA), $Ld \approx \infty$
- Pumping rate: $g_0(r_h = 4\text{UA}, \dot{r_h} = +18.7\,\text{km/s}) = 1.08{\times}3.08{\times}10^{-20}$W/molecule
- $$L/N_{rh} = \frac{g_0}{r_h^2} = 0.233 \times 10^{-20}\text{W/molecule}$$
- Spectrum: Slit of 2.4", from a line of 0.82" (1 pixel) at ρ=80000 km from center
- $$S = 1.34 \times 10^{13}\text{m}^2$$
- CN line: peak at 23×10^{-17}erg cm^{-2}s^{-1}Å^{-1} = 2.3×10^{-19}W m^{-2}Å^{-1}
- Integrated flux of the line (≈25Å): $F = 5.6 \times 10^{-18}$W m^{-2} (Fig. b upper right)
- $$L = 4\pi\Delta^2\ F = 2.1 \times 10^7\text{W}$$

Hence, the column density: $N(\rho = 80000\text{km}) = 6.7 \times 10^{14}\text{m}^{-2}$
$N(\rho) = \frac{Q_{\text{CN}}}{2\pi\ v_{gaz}\ \rho} \int_0^{\rho/Lp} K_0(x)dx \Rightarrow N(80000\text{km}) \approx 0.7 \times \frac{Q_{\text{CN}}}{3.3{\times}10^{11}} = 2.1 \times 10^{-12} Q_{\text{CN}}$
So we get Q_{CN}(Hale-Bopp on 19/12/1997) = 3.1×10^{26} molecules per second.

Within 2 AU from the Sun CN/H_2O≈0.2% in most cases. So we can extrapolate to a total outgassing rate around 1.7×10^{29} water molecules per second (If not measuring OH) which is about 5 tones per second. In fact, at this distance (3.8 AU) HCN is much more volatile than H_2O and we had $Q_{\text{H}_2\text{O}} = 2.8 \times 10^{28}$ molec.s^{-1} ([11]).

5 The observation of dust

Observation of dust may not be as relevant to cometary spectroscopy, but we will just quickly mention it here. Dust signal does depend on wavelength, especially as in the visible one must also avoid confusion with gas spectral features. In the infrared there are event dust (e.g. silicates) spectral features to identify, although beyond reach of amateur equipment.

5.1 Distribution of dust

The behavior of dust is somewhat more complicated than molecules, and we will first assume the simpler case where:

- dust emission is uniform and isotropic (no significant jets);
- dust velocity is constant;
- dust grains do not fragment into smaller ones,...;
- radiation pressure effect is negligible (i.e. relatively close to the nucleus).

In this case we can give a density profile following the Haser formalism:
$n_{\rm dust}(r) = \frac{Q_{\rm dust}}{4\pi\ r^2\ v_{dust}}$ $\Rightarrow$ $N(\rho) = \frac{Q_{\rm dust}}{4\ v_{dust}}\frac{1}{\rho}$

In the reality dust grains are not of unique size and velocity and they can be described with a distribution law: typically the number of grains $n(a)$ of size a increases as a^{-4} – $a^{-3.5}$ to $a^{-4.6}$, considering grains larger than 0.1μm. The grain velocity also depends on the sizes: $v_{\rm dust}(a < 1\mu{\rm m}) \approx v_{\rm gas} \approx 750$ m s^{-1} $v_{\rm dust}(a \approx 200\mu{\rm m}) \approx \frac{v_{\rm gas}}{10}$.
Most of the dust grains seen in the visible are in the $a = 0.1$ to 10μm size range. What will be noticed first on the dust images are the departure from the above $N(\rho) \propto \frac{1}{\rho}$ law, due to radiation pressure and jets effects.

5.2 In the far infrared

As Fig.1 and 2 show, observation of cometary comae in the mid- to far infrared reveals the dust grain thermal emission. Several well calibrated measurements on a wide range of wavelength can be used to measure the black body equivalent temperature of the grains, typically in the 150-400 K range. It can also be used to evaluate the total dust mass present in the cometary coma and dust loss rate of the nucleus $Q_{\rm dust}$. Since these are performed at a quite different wavelength such measurements are very complementary to visible measurements: they are sensitive to the emissivity and different size domain of the dust particles. Finally dust spectral features can be identified:

- Silicates emission bands at $10\mu m$ and $20\mu m$, whose shapes are sensitive to the ratio of crystalline to amorphous silicates as well as relative abundances of the various forms of silicates (olivine, pyroxene);
- Far from the Sun, water ice absorption bands in the dust grain coma have also been identified (1.5, $2.04\mu m$) in some active comets.

5.3 In the visible

Cometary dust scatters the solar light. Mie theory can be used to evaluate the scattering efficiency: roughly the larger particles ($a > \lambda$, wavelength) will scatter incoming solar light with an efficiency proportional to $1/\lambda$, while in the case of the smaller particles, it will be proportional to $1/\lambda^4$ following Rayleigh scattering rules.

What can be measured is the reddening (in % variation of the continuum per Å) of the comet dust continuum spectrum in comparison to the incoming solar emission, and its spatial variation. It usually reveals the physical properties of the dust grains. For example, in the case of grain fragmentation as they move away from the nucleus, size distribution will change radially and so can the reddening.

Afρ : This parameter has been invented decades ago by Mike A'Hearn ([1]) to get a parameter easy to measure in order to characterize the dust radiation flux of a comet observed in (any) given photometry aperture. In principle this parameter is a quantity easy (non model dependent) to measure and should be related to the dust production rate. It is measured on a circular aperture (projected radius on the sky ρ) – preferred to rectangular $x \times y$ window – centered on the nucleus. Afρ = albedo × filling factor of cometary dust (1 would mean it is fully opaque throughout the field of view selected) × field radius. Since we saw that $N(\rho) \propto 1/\rho$ then $f \propto \frac{\int N(\rho')\rho' \ d\rho' \ d\theta}{\pi\rho^2}$ is proportional to $1/\rho$. So Afρ should not depend on the aperture size on which it is measured and be proportional to the total dust production rate $Q_{\rm dust}$.

In practice, the parameter is evaluated on the calibrated data by: $Af\rho = \frac{\rm Scattered-flux}{\rm Incoming-solar-flux} \times \rho$, hence the formulae:

$$Af\rho = \frac{4\times\pi\Delta^2 \ F}{\pi\times\rho^2 \frac{F_{sun}}{r_h^2}} \times \rho = \frac{(2\Delta \ r_h)^2}{\rho}\frac{F}{F_{sun}} \qquad \text{or } Af\rho \approx \frac{(2\Delta \ r_h)^2}{x\times y/(\pi\rho')}\frac{F(\rho')/2}{F_{sun}}$$

Where Δ, r_h, ρ, ρ', x, y are in [m], F in [Wm^{-2}], (F_{sun} = solar flux at 1 AU). ρ' is the offset from center and $x \times y$ the rectangular aperture for the approximated formula given by [8].

The Afρ is the parameter commonly published in scientific publications as the observed quantity, while one would be more interested in the total dust (mass) production rate $Q_{\rm dust}$ to derive the dust-to-gas ratio of the comet. This later one will depend on the modeling, including several parameter as regards to dust properties (size distribution, velocity, albedo,...) not well characterized.

6 What to do with visible cometary spectra?

This section summarizes the main interests of visible cometary spectroscopy.

6.1 Measurable Quantities

- When doing spectro-imaging (with a slit): spatial distribution of the molecules and first "qualitative" molecule to molecule or molecule to dust spatial extent comparison;
- Next step is measurement of the molecules (radicals) scale-lengths: "*Lp*" and "*Ld*", cf section 4.1;
- Comparison between comets of the relative line intensities and lines relative to continuum (e.g. C_2/CN, C_3/CN lines ratios, C_2/dust). In a semi-quantitative way this will tell us quickly about the main characteristics of the comet: C_2 and C_3 depleted or not (cf example in Figs. 13), large dust to gas ratio or not,...;
- measurement of the dust reddening (% per Å) throughout the coma.

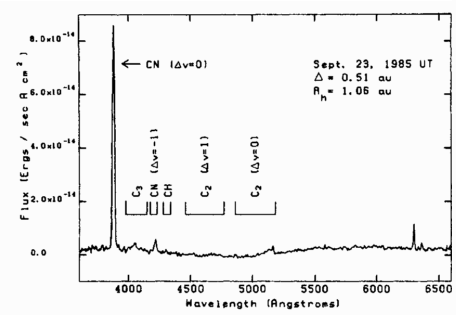

FIG. 1. Spectrum of Comet Giacobini-Zinner obtained 23 September 1985. The most important molecular features are marked. Note the low intensity of the C_2 and C_3 features relative to the CN features.

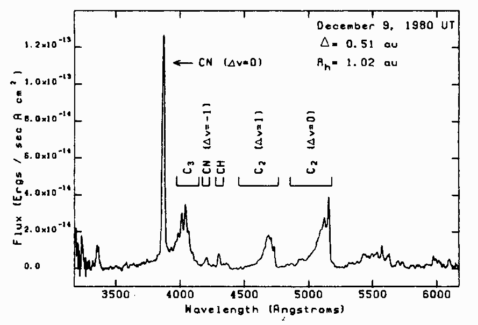

FIG. 2. Spectrum of Comet Tuttle obtained 9 December 1980. This spectrum was obtained at approximately the same heliocentric and geocentric distances as the Giacobini-Zinner spectrum shown in Fig. 1. Note the difference in the C_2 and C_3 molecular emission strengths compared to Fig. 1.

Fig. 13. Two cometary spectra obtained in very similar conditions but showing two comets that have a quite different C_2/CN ratio [7]

6.2 Useful to necessary corrections to make reliable comparisons

In a second step, one should do some corrections before making more quantitative comparisons:

- Geometrical effects must be taken into account: Δ the distance to the Earth must be used to convert measured values into physical units [m], and r_h the heliocentric distance is also a parameter on which several parameters such as scale-lengths depend (as r_h^2 or $r_h^{1.5}$ when not evaluated from the observation) – to take into account before quantitative comparisons;
- After taking into account heliocentric distance, one should correct the variation of the pumping rate with **heliocentric velocity** of the comet, in the case of OH and CN, following tables in [21] and [23], e.g., in order to compare observations done at different dates or with different comets;
- Finally, from the first step of obtaining a well calibrated spectra (photometrically calibrated data after correction for the various efficiencies of the system, getting rid of night sky lines, using photometric standard stars,...), converting data into molecular production rates and relative abundances.

If one reaches this last step, then a quantitative comparison between comets is feasible as well as following the evolution of comet with time, distance to the Sun,...

6.3 With clean (calibrated) data or bigger equipment:

Obtaining data of high scientific value is certainly within reach of an experienced observer, well equipped and careful about data acquisition and calibration. At this point data of high scientific value (even of use to the professional community) can be obtained and published:

- Measurements of molecular scale-lengths on the spectro-images: they do not require well photometrically calibrated data, but good quality with good signal-to-noise and some calculation work;
- Precise production rate measurements, as presented in the previous section, but computation with a more sophisticated model of the line pumping process may be useful as a contribution from the professional side;

And finally, here are two aspects of cometary spectroscopy, which really require semi-professional to professional large equipment or experience:

- High resolution ($\lambda/\Delta\lambda > 10000$) spectroscopy and analysis of the fine structure of the bands, requiring sophisticated models;
- Very high resolution ($\lambda/\Delta\lambda > 60000$) comet spectroscopy that enables to isolate all individual lines of the rotational fine structure: this is required to further measure the ortho/para ratio in NH_2, the $C^{15}N/C^{14}N$, $^{13}CN/^{12}CN$,... ratios. (Note that the terrestrial ratios are $^{13}C/^{12}C$=1/93 and $^{15}N/^{14}N$ = 1/272). This has been only done with 8-m class telescopes on recent bright comets!

7 Conclusion

The most efficient spectroscopic techniques to study in detail cometary atmospheres are beyond amateurs means: radio and infrared requires large expensive equipment and even in the visible sensitive programs also require large equipment. But, on the other hand, the comet investigations in these domain are quite limited: the teams of scientists/observers are very small (on the order of 100 or so all over the world for all spectroscopic studies of comets) and corresponding observing time with the large facilities are limited.

Comets are variable targets and differ from each other, so that wide coverage in targets and time with less deep studies is also essential. Amateurs can play an essential role here: limited equipment (20cm class telescope with mid-to-low resolution optical spectrometer $R \approx 200 - 1000$) can be enough for a useful work. The experienced amateur careful about data quality and calibration can provide very valuable data, especially as very few professional would do the same. The radicals (C_2, C_3, CN, NH_2 up to OH in the near UV) that can be detected and are also very useful to monitor comet activity. We have seen that it is possible to retrieve quantitative information and the experienced amateur can also provide valuable information in a short time that professional community would appreciate to plan extensive investigations. In the future we can even expect professional–amateur collaborations to publish amateur work in scientific refereed publications.

References

1. A'Hearn, M.F.,
Astrophysical Journal **219**, 768–772, 1978

2. A'Hearn, M.F.,
in COMETS, ed. Laurel L. Wilkening, University of Arizona press, 433–460, 1982
3. A'Hearn, M.F., Millis, R.L., Schleicher, D.G., Osip D.J. & Birch, P.V.,
Icarus **118**, 223–270, 1995
4. Arpigny, C., Jehin, E., Manfroid, J., et al.,
Science **301**, 1522–1524, 2003
5. Biver, N.,
in "Interaction Rayonnement-Matière dans les atmosphères Planétaires et Cométaires", ed. G. Moreels, Published by Besançon Observatory, 205–216, 1996-2002
6. Bockelée-Morvan, D., Biver, N., Colom, P. et al.,
Icarus **169**, 113-128, 2004
7. Cochran, A.L. & Barker, E.S.,
Astronomical Journal **92**, 239–243, 1987
8. Cochran, A.L., Barker, E.S., Ramseyer, T.F. & Storrs, A.D.,
Icarus **98**, 151–162, 1992
9. Crovisier, J. & Encrenaz, T.,
"Les Comètes, Témoins de la Naissance du Système Solaire."
Belin-CNRS Editions, 1995 (ISBN 2-271-05300-5 & 2-7011-1714-3)
10. Crovisier, J.,
in "Interaction Rayonnement-Matière dans les atmosphères Planétaires et Cométaires", ed. G. Moreels, Published by Besançon Observatory, 137–155, 1996-2002
11. Crovisier, J.
in "Astrochemistry: From molecular Clouds to Planetary Systems"
IAU Symposium 197, Y.C. Mihn and E.F. van Dishoeck edts, ASP, 461–470, 2000
12. Festou, M.C. & Zucconi J.-M.,
Astronomy & Astrophysics **134**, L4–L6, 1984
13. Festou, M.C., Rickman, H. & West R.M.,
Astronomy & Astrophysics Review, **vol. 4, no. 4**, 363–447, 1993
Astronomy & Astrophysics Review, **vol. 5, no. 1-2**, 37–163, 1993
14. Kleine, M., Wyckoff, S., Wehinger, P. A. & Peterson, B. A.,
Astrophysical Journal **436**, 885–906, 1994
15. Laffont, C.,
"Etude d'émissions gazeuses dans les régions internes de 3 comètes: Halley, C/1996 B2 (Hyakutake) et C/1995 O1 (Hale-Bopp)" Université Paris 6, PhD. Thesis, 1998
16. Lecacheux, A., Biver, N., Crovisier, J., et al.,
Astronomy & Astrophysics **402** L55–L58, 2003
17. Meier, R., Wellnitz, D., Kim, S.J. and A'Hearn, M.F.,
"The NH and CH Bands of Comet C/1996 B2 (Hyakutake)" Icarus, **136**, 268–279, 1998
18. Mumma, M.J., McLean, I.S., DiSanti, M. A. et al.,
Astrophysical Journal **546**, 1183–1193, 2001
19. Rauer, H., Helbert, J., Arpigny, C. et al.,
Astronomy & Astrophysics **397**, 1109–1122, 2003
20. Rousselot, P., Arpigny, C., Rauer, H. et al.,
Astronomy & Astrophysics **368**, 689–699, 2001
21. Schleicher, D.G.,
"The fluorescence of cometary OH and CN"
University of Maryland, PhD thesis, 1983

22. Schleicher, D.G., Millis, R.L. & Birch, P.V.,
Astronomy & Astrophysics **187**, 531–538, 1987
23. Schleicher, D.G. & A'Hearn, M.F.,
Astrophysical Journal **331**, 1058–1077, 1988
24. Schleicher, D.G., Millis, R.L. & Osip D.J.,
Icarus **94**, 511–523, 1991
25. Tegler, S.C., Campins, H., Larson, S. et al.,
Astrophysical Journal **396**, 711–716, 1992
26. Weaver, H.A. and Feldman, P.D.
in " Science with the Hubble Space Telescope", Eds. P. Benvenuti and E. J. Schreier,
ESO Conference and Workshop Proceedings **44**, 475, 1992
27. *Proceedings of the first international conference on comet Hale-Bopp:* Earth, Moon and Planets **78**, (Kluwer Academic Publishers) 1997-1999
28. *Proceedings of the first international conference on comet Hale-Bopp:* Earth, Moon and Planets **79**, (Kluwer Academic Publishers) 1997-1999
29. *Proceedings of the international conference "Cometary Science after Hale-Bopp":* Earth, Moon and Planets **89**, (Kluwer Academic Publishers) 2002
30. *Proceedings of the international conference "Cometary Science after Hale-Bopp":* Earth, Moon and Planets **90**, (Kluwer Academic Publishers) 2002